A new technique for high precision sub-regional camera calibration based on checkerboard pattern

SHEN Xin-lan, WANG Zhong, LIU Chang-jie, FU Lu-hua

(*State Key Laboratory of Precision Measuring Technology and Instruments, Tianjin University, Tianjin 300072, China*)

Abstract: Camera calibration is critical in computer vision measurement system, affecting the accuracy of the whole system. Many camera calibration methods have been proposed, but they cannot consider precision and operation complexity at the same time. In this paper, a new technique is proposed to calibrate camera. Firstly, the global calibration method is described in detail. It requires the camera to observe a checkerboard pattern shown at a few different orientations. The checkerboard corners are obtained by Harris algorithm. With direct linear transformation and non-linear optimal algorithm, the global calibration parameters are obtained. Then, a sub-regional method is proposed. Those corners are divided into two groups, middle corners and edge corners, which are used to calibrate the corresponding area to get two sets of calibration parameters. Finally, some experimental images are used to test the proposed method. Experimental results demonstrate that the average projection error of sub-region method is decreased at least 16% compared with the global calibration method. The proposed technique is simple and accurate. It is suitable for the industrial computer vision measurement.

Key words: sub-regional camera calibration; computer vision; checkerboard pattern

CLD number: TM930.1 **Document code**: A

Article ID: 1674-8042(2016)04-0342-08 **doi**: 10.3969/j.issn.1674-8042.2016.04.006

0 Introduction

Non-contact detection technique based on computer vision is increasingly applied in the field of industrial automation because of its high precision, speed, etc. In computer vision measurement system, camera calibration accuracy is critical which can affect the accuracy of the whole system[1-3]. In workpiece detecting system based on computer vision, images of workpieces can be collected by a CCD camera. Through a series of image processing algorithms, geometrical parameters of workpieces are obtained. Comparing with the standard parameters, those workpieces are divided into two groups, qualified and unqualified[4]. Fig. 1 shows a workpiece to be measured. There are datums of hole C and plane B in the workpiece. Drawing a line from hole C to plane B, a unified coordinate system is established. Then it is easy to achieve geometrical parameters of the workpiece such as verticality, flatness, symmetry, etc. Camera calibration is absolutely necessarily technique for obtaining the world coordinates of hole C. It is essential to find out a high precision camera calibration technique.

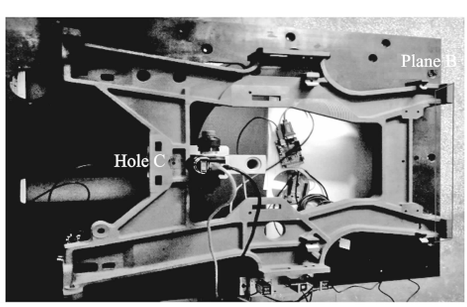

Fig. 1 A workpiece to be measured

The existing techniques for camera calibration can be classified into three categories, traditional calibration techniques, self-calibration techniques and cali-

Received date: 2016-10-15

Foundation items: Tianjin Research Program of Application Foundation and Advanced Technology (No. 14JCYBJC18600, No. 14JCZDJC39700); the National Key Scientific Instrument and Equipment Development Project (No. 2013YQ17053903)

Corresponding author: SHEN Xin-lan (shenxinlan_1991@163.com)

bration techniques based on active vision. Traditional calibration techniques[5-6] require size of calibration object known, and its imaging model and optimization algorithm have been very mature, but limited to the applications. Self-calibration techniques[7,8] do not use any calibration object. Just by moving a camera in a static scene, the rigidity of the scene provides in general two constraints on the cameras' internal parameters from one camera displacement by using image information alone. These techniques have high flexibility, but poor robustness. Calibration techniques based on active vision[9-10] use some known camera motion information to calibrate camera. The relevant algorithms are simple. Their linear solutions are often able to obtain, so they have strong robustness. However, they are not flexible enough because they need precise camera motion platform.

ZHANG Zhengyou proposed a flexible new technique to easily calibrate a camera[11]. The technique only needed a plannar pattern, which could be printed on a laser printer. The motion of the plannar pattern needed not to be known. The proposed procedure consisted of a closed-form solution, followed by a nonlinear refinement based on the maximum likelihood criterion. The technique lied between the traditional calibration and self-calibration. And it had been widely used because of its simple and flexible. Refs. [12-15] were based on Zhang Zhengyou calibration algorithm, they used all corners together to calibrate camera. They believed that the distortion parameters were the same in different regions in the image. Since the processing error of the camera and lens is inevitable, we can not guarantee that the distortion parameters are the same.

Ref. [16] presented the technique for sub-regional camera calibration based on moving light target. A round light target was moved with the coordinate measuring machine to obtain a set of accurate points. The image plane was separated into several sections according to the circle symmetrical structure. And camera parameters in different regions were calculated with the sub-regional points. Experiments demonstrated that the method was very accurate when the number of divided regions achieved a certain number. But it had to use a precise instrument to get the accurate points. The cost of the precise instrument was too expensive for most measuring systems, and it was complicate in operation.

Camera calibration methods mentioned above cannot consider precision and operation complexity at the same time. A novel approach is proposed to tackle the hard problem in this paper. The rest of this paper is organized as follow: section 1 describes two common camera model. Section 2 gives the global camera calibration method. Section 3 proposes a new technique for sub-regional camera calibration. Section 4 provides the experimental results. Both the global method and the sub-regional method are used to calibrate the camera. Finally, Section 5 concludes this paper.

1 Camera model

1.1 Distortion-free camera model

Distortion-free camera model is a pinhole camera model that neglects all optical distortion. It is related to four kinds of coordinates[17], world coordinate system ($O_W-X_WY_WZ_W$), camera coordinate system ($O_C-X_CY_CZ_C$), image coordinate system (O_i-xy), pixel coordinate system (O_p-uv), as shown in Fig. 2.

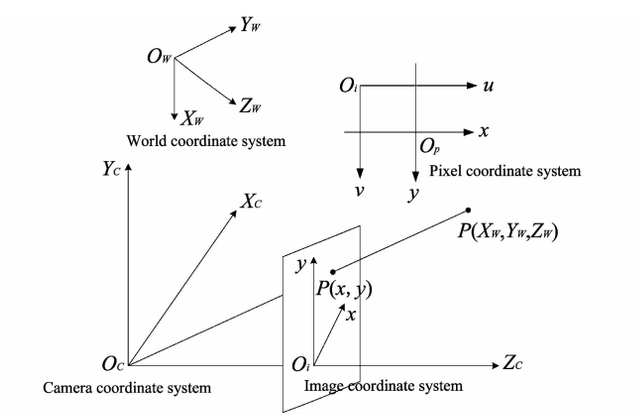

Fig. 2 Four kinds of coordinates system

The relationship between world coordinate system and pixel coordinate system is

$$\rho\begin{bmatrix}u\\v\\1\end{bmatrix}=\begin{bmatrix}f/\mathrm{d}x & 0 & u_0 & 0\\ 0 & f/\mathrm{d}y & v_0 & 0\\ 0 & 0 & 1 & 0\end{bmatrix}\begin{bmatrix}\boldsymbol{R} & \boldsymbol{t}\\ \boldsymbol{0}^{\mathrm{T}} & 1\end{bmatrix}\begin{bmatrix}X_W\\Y_W\\Z_W\\1\end{bmatrix}=\boldsymbol{M}\begin{bmatrix}\boldsymbol{R} & \boldsymbol{t}\\ \boldsymbol{0}^{\mathrm{T}} & 1\end{bmatrix}\begin{bmatrix}X_W\\Y_W\\Z_W\\1\end{bmatrix}, \tag{1}$$

where ρ is a scale factor, f is the focal length, $\mathrm{d}x$ and $\mathrm{d}y$ is the pixel distance between the adjacent pixels in x and y direction. (u_0, v_0) is intersection point of main optical axis and image plane. These parameters are determined by the internal structure of the camera, called the internal camera parameters. $\boldsymbol{M}$ is internal parameter matrix. $\boldsymbol{R}$ is a 3×3 orthogonal rotation matrix, $\boldsymbol{t}$ is a three-dimensional translation vector. $\mathbf{0}^{\mathrm{T}}$ represents the matrix $(0,0,0)^{\mathrm{T}}$. $\boldsymbol{R}$ and $\boldsymbol{t}$ are called the external camera parameters because they are determined by the relative position of the camera coordinate system and the world coordinate system.

1.2 Distortion camera model

In practice, a camera usually exhibits significant lens distortion. Then the distortion-free camera model can not hold true, and it must take into account the distortion. As shown in Fig. 3, $P_d(x_d, y_d)$ is the distortion-free coordinate, and $P_u(x_u, y_u)$ is the corresponding coordinate with distortion.

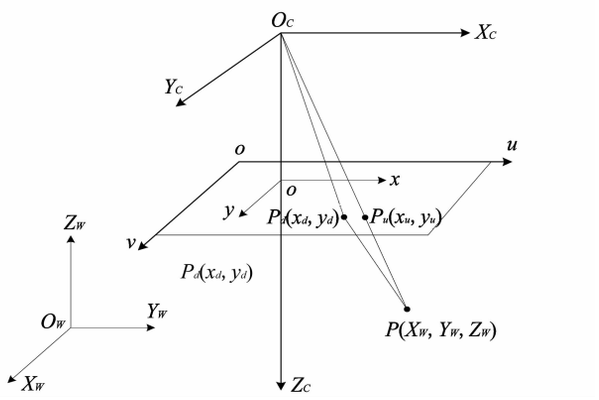

Fig. 3 Distortion camera model

There are three major kinds of distortion, radial distortion, decentering distortion and thin prism distortion[18]. Radial distortion is mainly caused by flawed radial curvature curve of the lens elements. The others are generally caused by improper lens and camera assembly, and generate both radial and tangential errors.

In this paper, we consider radial and tangential distortion. The relationship between $P_d(x_d, y_d)$ and $P_u(x_u, y_u)$ is

$$\begin{cases} x_u = x_d(1+k_1r^2+k_2r^4)+[2p_1y_d+p_2(r^2+2x_d^2)], \\ x_u = y_d(1+k_1r^2+k_2r^4)+[p_1(r^2+2y_d^2)+2p_2x_d], \end{cases} \tag{2}$$

where k_1, k_2 are radial distortion parameters; p_1, p_2 are tangential distortion parameters; r represents the distance between (x_d, y_d) and (u_0, v_0); k_1, k_2, p_1, p_2 also belong to the internal parameters of the camera.

2 Global camera calibration

2.1 Image acquisition

Taking a few images of the checkerboard plane under different orientations by moving the plane, the number of images must be enough to solve meaningful calibration parameters. Supposing that the checkerboard plane has N corners, and K images of the plane in different positions can be collected. Every position has three rotation parameters and three translation parameters, and they share four internal parameters. The number of parameters to be solved is $6K+4$. Each corner has two coordinate values, x and y. $2NK$ constraint conditions can be obtained. Therefore, in order to solve the calibration parameters, the condition must be satisfied: $2NK \geqslant 6K+4$.

2.2 Corner detection

Camera calibration methods based on checkerboard plane use coordinates of corners to build the relationship between the three-dimensional world and the two-dimensional image. The existing algorithm for corner detection can be divided into two categories[19]. The first one seeks the intersections of contour lines. It depends on the image edge extraction effect and has large computation, and it is used in a small range. The second one is based on the change of the gray of a image, such as Harris operator, Susan operator, etc. Harris operator has good positioning performance and robustness. And its algorithm is simple and stable. It is one of the most widely used of the corner detection algorithms[20]. Harris operator is used in this paper to detect corners.

The principle of Harris algorithm is that the gray of a corner will change greatly when the corner move in any direction. A small window can be used to observe the gray change of a point. Then it is easy to know whether the point is a corner.

The gray change of a point is related to the matrix

$\boldsymbol{G}$, $\boldsymbol{G}$ is defined as

$$\boldsymbol{G} = \begin{bmatrix} I_x * I_x & I_x * I_y \\ I_x * I_y & I_y * I_y \end{bmatrix}, \tag{3}$$

where I_x, I_y represent gray gradient of the point in horizontal and vertical direction.

The response function value H of the point can be computed by

$$H = \mathrm{Det}(\boldsymbol{G}) - k * trace(\boldsymbol{G})^2, \tag{4}$$

where k is an empirical value. The point is a corner when H is greater than the given threshold.

The coordinates of corners are pixel level by Harris algorithm. In order to improve accuracy of subsequent calibration, it is necessary to achieve the sub-pixel coordinates of corners. The vector between the sub-pixel corner and the surrounding pixels should be perpendicular to the gray gradient. Then the sub-pixel coordinates of corners can be calculated by an iterative approach of minimizing the error function[21].

2.3 Parameter solution

The internal and external camera parameters can be calculated in two steps. Firstly, regardless of the distortion, the initial camera calibration parameters can be obtained through direct linear transformation. This step is fast, but these parameters are not accurate. Secondly, we can establish a objective function while considering the distortion. The function is defined as

$$F = \sum_{i=0}^{NK} (u_i - u_i')^2 + \sum_{i=0}^{NK} (v_i - v_i')^2, \tag{5}$$

where (u_i, v_i) is actual pixel coordinate of the corner i, and (u_i', v_i') is theoretical pixel coordinate, which is obtained by projecting the corner i to the pixel plane based on the distortion model. The initial distortion parameters are taken as 0. Through the nonlinear optimal algorithm, the final internal and external camera parameters can be obtained after several times of iteration[22].

3 Sub-regional camera calibration

It was proved that the main actor of affecting distortion is radial distortion in Ref. [23]. The existing camera calibration methods mainly consider the radial distortion, ignoring other non-linear distortion. According to the formation principle of the radial distortion, distortion of the middle points is small, and distortion of the edge points is large. If the same distortion parameters are used in the entire image, it will cause distortion parameters overvalued in the middle region and undervalued in the edge region. A technique is proposed for sub-regional camera calibration based on checkerboard pattern in this paper.

3.1 Regional division principle

The sub-regional thought is based on the checkerboard pattern rather than the entire image. In the procedure of collecting images, the checkerboard pattern is placed in some proper positions to fill the whole field of view. And the center of the checkerboard is adjusted to close the center of the whole image as possible. According to the relative position between corners and the center of the whole image, corners of the checkerboard pattern are divided into two groups, middle corners and edge corners. We can suppose that there is n middle corners and $(N-n)$ middle corners, so two conditions must be satisfied: $2nK \geqslant 6K+4$ and $2(N-n)K \geqslant 6K+4$.

3.2 Average projection error

The camera calibration accuracy can be measured by the average projection error of the images. At first, the world coordinates of corners are projected onto the two-dimensional image plane, so the theoretical pixel coordinates of corners can be obtained. Then the average projection error of each image in x and y direction can be calculated by subtracting the theoretical pixel coordinates from the practical pixel coordinates on average. As for sub-regional methods, two sets of calibration parameters can be obtained. In order to obtain the average projection error of the whole image, it is necessary to combine the two sets of calibration parameters. The specific method is as follow: the calibration parameters of the internal and external camera parameters of the middle region are applied to all corners to obtain projection error of every corner in x and y direction, but only projection error of the middle corners is valid. Similarly, projection error of every corner can be calculat-

ed by the calibration parameters of the edge region, but only projection error of the edge corners is valid. Finally, two sets of valid projection error are combined to figure out the average projection error of the whole image.

4 Experiments and analysis

The size of the checkerboard used in the experiment is 60 mm×60 mm. The length and width of each grid is 4 mm. Eight images are collected by the industrial camera MV-VEM500SM and the industrial lens AF-2514MP of the Microvision company, as shown in Fig. 4. The maximum resolution of the camera is 2 592×1 944. It is set to 1 024×768 in order to make the checkerboard fill the whole field of view.

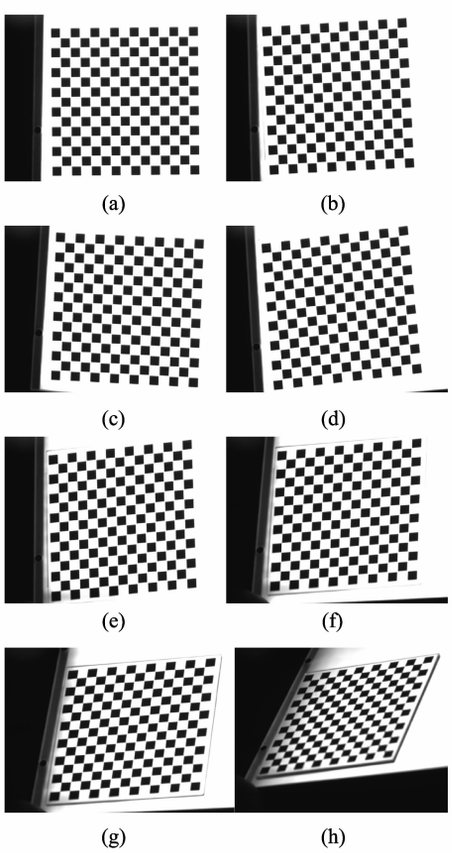

Fig. 4 Eight original images

4.1 Corner detection results

In the experiment, Harris algorithm is used to detecte corners in each image. Considering the outermost corner closed to the edge of a image, it is excluded for calibration. The results are shown in Fig. 5, and a black solid points represents a corner.

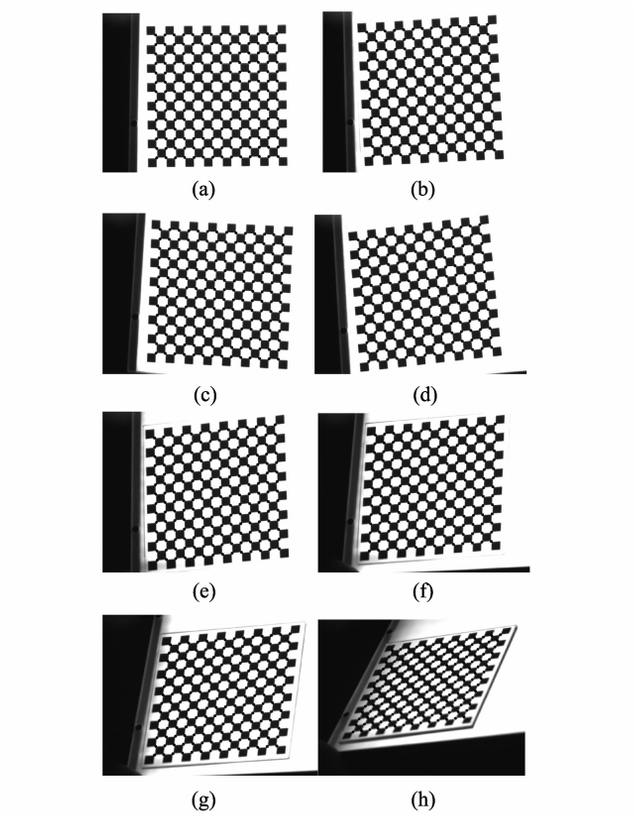

Fig. 5 Corner detection results

4.2 Global calibration results

Using coordinates of all corners obtained in 4.1, the global calibration parameters are solved by direct linear transformation and non-linear optimal algorithm, as shown in Table 1 and Tables 2(a)—(b).

Table 1 Internal parameters of global calibration

Internal parameters	Value
$f/\mathrm{d}x$ (pixel)	12 363.233 40
$f/\mathrm{d}y$(pixel)	12 373.835 94
u_0(pixel)	587.986 63
v_0(pixel)	455.992 58
k_1	−0.503 28
k_2	−89.666 07
$p_1(/10^{-3})$	1.678 08
$p_2(/10^{-3})$	1.684 59

Table 2(a) External parameters of global calibration

External parameters	Image label			
	a	b	c	d
r_1	−0.016 79	−0.077 79	−2.066 90	−0.157 92
r_2	−3.132 59	−2.926 83	−2.159 37	−2.980 82
r_3	0.004 13	0.006 06	−0.025 33	0.272 04
$t_1(/10^{-1})$	2.300 30	1.768 59	−2.681 67	1.822 97
$t_2(/10^{-1})$	−3.127 45	−3.410 92	−3.295 94	−3.513 63
$t_3(/10^{-3})$	1.086 51	1.072 75	1.077 63	1.069 76

Table 2(b) External parameters of global calibration

External parameters	Image label			
	e	f	g	h
r_1	−0.090 59	−0.029 41	0.026 480	0.141 68
r_2	−2.823 46	−2.785 66	−2.679 88	−2.381 23
r_3	0.334 85	0.568 77	0.736 95	1.125 66
$t_1(/10^{-1})$	2.005 64	2.293 48	2.579 28	2.633 82
$t_2(/10^{-1})$	−3.362 33	−3.429 19	−3.087 48	−3.192 36
$t_3(/10^{-3})$	1.058 35	1.053 66	1.046 74	1.035 44

4.3 Sub-regional calibration results

The number of corners used in the experiment is 196(14×14). Combined with regional division principle, we use three different sub-regional methods. The numbers of the middle corners of three methods are 6×6, 7×7, 8×8, respectively, as shown in Fig. 6.

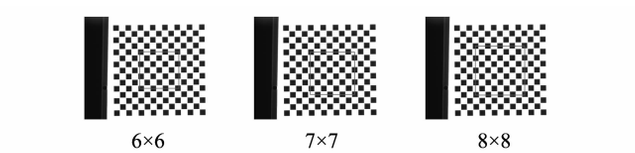

Fig. 6 Three sub-regional methods

Combined with direct linear transformation and non-linear optimal algorithm, two group corners are used to calibrate the corresponding area to get two sets of calibration parameters. The internal parameters of the three sub-regional methods are shown in Tables 3(a)−(b).

Table 3(a) Internal parameters of the sub-regional methods

Internal parameters	Sub-regional calibration methods		
	6×6 middle	6×6 edge	7×7 middle
f/dx (pixel)	12 667.964 84	12 396.433 59	11 865.211 91
f/dy (pixel)	12 684.958 01	12 405.759 77	11 869.524 41
u_0(pixel)	512.365 11	674.849 61	591.339 60
v_0(pixel)	384.512 79	417.541 75	293.151 15
k_1	−0.719 44	−0.907 65	−0.779 06
k_2	−0.107 25	126.776 49	−0.025 15
$p_1(/10^{-3})$	4.351 10	3.262 24	7.596 56
$p_2(/10^{-3})$	8.526 11	−0.435 77	−0.577 58

As shown in Tables 3(a)−(b), no matter what kind of sub-regional methods we use, the absolute values of radial distortion parameters in the middle region are significantly smaller than the absolute value of radial distortion parameters in the edge region. In addition, compared with the global calibration, the absolute values of radial distortion parameters in the middle region with the two sub-regional methods (6×6 and 7×7) are smaller, and the absolute values of radial distortion parameters in the edge region with the two sub-regional methods (6×6 and 7×7) are larger.

Table 3(b) Internal parameters of the sub-regional methods

Internal parameters	Sub-regional calibration methods		
	7×7 edge	8×8 middle	8×8 edge
f/dx (pixel)	12 389.110 35	12 229.138 67	12 404.095 70
f/dy (pixel)	12 398.574 22	12 239.959 96	12 413.602 54
u_0(pixel)	692.743 04	655.825 93	690.110 47
v_0(pixel)	444.421 45	500.418 43	433.597 56
k_1	−0.865 71	−0.455 46	−0.928 71
k_2	103.995 25	126.469 76	128.268 84
$p_1/(10^{-3})$	2.949 24	3.819 37	3.331 17
$p_2/(10^{-3})$	−0.432 53	1.533 40	−0.426 71

4.4 Comparative analysis

Figs. 7 and 8 show the projection error of each image in x and y direction with different calibration methods. It is obvious that the average projection error of each image with sub-regional methods is smaller than that of the global method. The average projection error of 8 images is shown in Table 4. Table 4 shows the average projection error of 8 images with different calibration methods. The performance of the global method is the worst in four methods of calibration. Compared with the global method, error of the three sub-regional method is reduced. The average projection error of 8 images with the sub-regional method 7×7 is reduced by about 61% in x direction, and about 57% in y direction. The average projection error of 8 images with the sub-regional method 8×8 is reduced by about 31% in x direction, and about 16% in y direction.

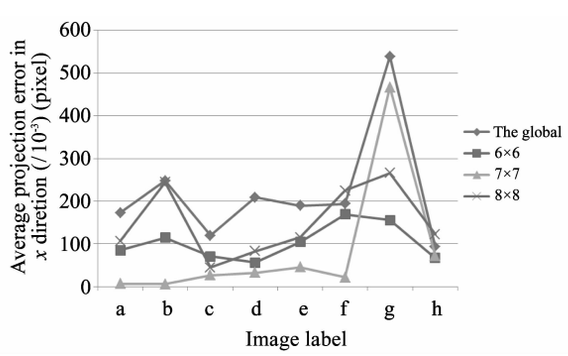

Fig. 7 Projection error of each image in x direction

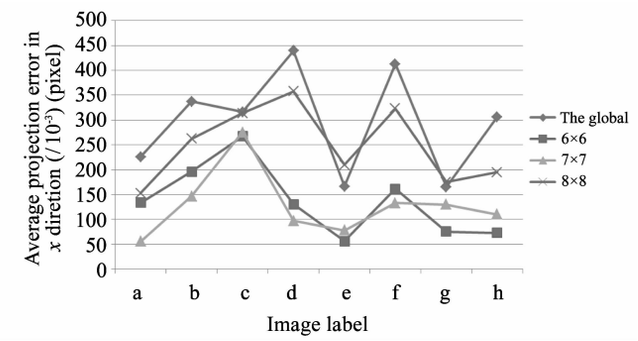

Fig. 8 Projection error of each image in *y* direction

Table 4 Average projection error of 8 images

Calibration method	In x direction (pixel)	In y direction (pixel)
Global	0.220 51	0.296 15
6×6	0.102 89	0.136 63
7×7	0.084 61	0.128 29
8×8	0.150 96	0.148 27

5 Conclusion

In this paper, a new technique is proposed to calibrate camera. The technique requires the camera to observe a checkerboard pattern from a few different orientations. With Harris algorithm, the checkerboard corners are easily obtained. The global calibration parameters are solved by linear transformation combined with non-linear optimal algorithm. Then a sub-regional method is proposed. Those corners are divided into two groups, middle corners and edge corners. The two groups are used to calibrate the corresponding area to achieve two sets of calibration parameters. In the experiment, very good results have been obtained. Comparing with the global calibration method, the average projection error of images by sub-region method is decreased at least 16%. The proposed technique is simple and precise. It is suitable for the industrial vision measurement.

References

[1] FENG Huan-fei. Research on camera calibration method in 3D reconstruction. Chongqing: Chongqing Jiaotong University, 2013: 9-12.

[2] LU Hong-liang. Camera calibration method for machine vision. Shenyang: Shenyang University of Technology, 2013: 10-14.

[3] HUANG Chun-yan. The extraction of depth information about the object based on binocular vision. Taiyuan: North University of China, 2015: 9-12.

[4] WU Xiao-liang. Research of workpiece 3D size measurement based on machine vision. Chengdu: Southwest Jiaotong University, 2013: 10-12.

[5] LI Peng, WANG Jun-ning. Overview of Camera Calibration methods. Shanxi Electronic Technology, 2007, 4: 77-79.

[6] Tsai R Y. An efficient and accurate camera calibration technique for 3D machine vision. Proc. ieee Conf. on Computer Vision & Pattern Recognition, 1986: 364-374.

[7] MENG Xiao-qiao, HU Zhan-yi. Recent progress in camera self-calibration. Acta Automatica Sinica, 2003, 29(1): 110-124.

[8] Maybank S J, Faugeras O D. A theory of self-calibration of a moving camera. International Journal of Computer Vision, 1992, 8(2): 123-151.

[9] Ma S D. A self-calibration technique for active vision systems. IEEE Transactions on Robotics & Automation, 1996, 12(1): 114-120.

[10] Quan L, Kanade T. Affine structure from line correspondences with uncalibrated affine cameras. Pattern Analysis & Machine Intelligence IEEE Transactions on, 1997, 19(8): 834-845.

[11] ZHANG Zheng-you. A flexible new technique for camera calibration. IEEE Transactions on Pattern Analysis & Machine Intelligence, 2000, 22(11): 1330-1334.

[12] LIU Yan, LI Teng-fei. Research of the improvement of Zhang's camera calibration method. Optical Technology, 2014, 40(6): 565-570.

[13] LI li. Camera calibration algorithm based on Open CV and improved Zhang Zhengyou algorithm. Light Industry Machinery, 2015, 33(4): 60-63, 68.

[14] WANG Dong, XIA Yi, YIN Mu-yi, et al. Camera calibration method based on OpenCV. Modern Electronics Technique, 2013, (8): 97-100.

[15] LI Hong-lei, GUAN Qun, HU Kai-heng, et al. Development of camera calibration system based on OpenCV in VC++ environment. Computer Applications and Software, 2011, 28(6): 19-21, 31.

[16] LIU Shu-gui, JIANG Zhen-zhu, DONG Ying-hua, et al. Sub-regional camera calibration based on moving light target. Optics and Precision Engineering, 2014, 22(2): 259-265.

[17] WANG Jian-hua, FENG Fan, LIANG Wei, et al. Nonlinear model based camera calibration. Optoelectronic Technique, 2012, 32(1): 33-38.

[18] Weng J, Cohen P, Herniou M. Camera calibration with distortion models and accuracy evaluation. IEEE Transac-

tions on Pattern Analysis and Machine Intelligence, 1992, 14(10): 965-980.

[19] WANG Xiao-hui, CHENG Jian-qing, HAN Yu. Improved checkerboard corner detection algorithm based on the Harris. Electronic Measurement Technology, 2013, 36(10): 51-54, 66.

[20] ZHANG Yu, FANG Kang-ling, LIU Yong-xiang. Harris algorithm-based corner detection on black white checkerboard. Computer Application and Software, 2010, 27(8): 251-254.

[21] LIANG Zhi-min, GAO Hong-ming, WANG Zhi-jiang, et al. Sub-pixels corner detection for camera calibration. Transactions of the China Welding Instruction, 2006, 27(2): 102-104, 118.

[22] YIN Wen-sheng, LUO Yu-lin, LI Shi-qi. Camera calibration based on OpenCV. Computer Engineering and Design, 2007, 28(1): 197-199.

[23] TIAN Yuan-yuan, HUANG He-cheng. Research on radial distortion based on CCD camera. World Sci-Tech R&D, 2008, 30(2): 168-170.

一种基于棋盘格的高精度分区域相机标定方法

申心兰，王　仲，刘常杰，付鲁华

（天津大学 精密测试技术及仪器国家重点实验室，天津 300072）

摘　要： 在视觉测量系统中，相机的标定精度至关重要，将影响整个测量系统的精度。针对现有相机标定方法难以兼顾精度和操作复杂度的问题，本文提出了一种基于棋盘格的高精度分区域相机标定方法。首先，将棋盘格置于不同位置，提取不同位置角点的世界坐标和像素坐标，对所有角点用线性变换和非线性最优算法求解出全局标定参数。然后，将角点分为中间区域角点和边缘区域角点，对两区域角点分别标定得到两组分区域标定参数。标定实验结果表明：与全局标定法相比，分区域标定法的图像平均投影误差至少降低16%。该方法操作简单，精度高，可以很好的应用于工业视觉检测。

关键词： 分区域相机标定；视觉测量；棋盘格

引用格式： SHEN Xin-lan, WANG Zhong, LIU Chang-jie, et al. A new technique for high precision sub-regional camera calibration based on checkerboard pattern. Journal of Measurement Science and Instrumentation, 2016, 7(4): 342-349. [doi: 10.3969/j.issn.1674-8042.2016.04.006]